A Review of System Calibration in the PEA Method Used for Space Charge Measurement

Yu, X.; Lagerweij, G.; Vaessen, P.; Mor, A. R.; Niasar, M. G.

DOI
10.1109/CEIDP61707.2025.11218436

Publication date
2025

Document Version
Final published version

Published in
Proceedings of the 2025 IEEE Conference on Electrical Insulation and Dielectric Phenomena (CEIDP)

A review of system calibration in the PEA method used for space charge measurement

Xuliang Yu[1], Gijs Lagerweij[2], Peter Vaessen[1,3], Armando Rodrigo Mor[4], Mohamad Ghaffarian Niasar[1]
[1]Department of Electrical Sustainable Energy, Delft University of Technology, Mekelweg 4, 2628 CD Delft, The Netherland
[2]Prodrive Technologies, Science Park Eindhoven 5501, 5692 EM Son, The Netherlands
[3]KEMA Laboratories, Klingelbeekseweg 195, 6812 DE Arnhem, The Netherlands
[4]Universitat Politècnica de València, Camino de Vera, s/n, 46022 Valencia, Spain

2025 IEEE Conference on Electrical Insulation and Dielectric Phenomena (CEIDP) | 979-8-3315-8902-8/25/$31.00 ©2025 IEEE | DOI: 10.1109/CEIDP61707.2025.11218436

***Abstract*- The PEA(pulsed electro-acoustic) method is widely used for measuring space charge distribution in insulation materials. However, the measured quantity reflects a voltage curve over time rather than the actual space charge distribution. Therefore, establishing a calibration procedure is crucial to determine the relationship between these two quantities. This calibration procedure aims to convert the measured voltage into the spatial distribution of space charge while correcting for non-idealities such as distortion and attenuation. This paper outlines the main steps of the PEA system calibration and provides a detailed discussion on the selection of the reference signal. Furthermore, recommendations are provided to enhance the accuracy and reliability of the calibration process.**

I. Introduction

PEA is a common method used to measure space charge distribution along one axis of an insulation material [1],[2]. Fig. 1 schematically shows a PEA setup for a flat sample. The dielectric sample is placed between two high-voltage electrodes. A polarization voltage will cause interface charges to accumulate between the sample and the electrodes. With the excitation of pulse voltage, internal charges already present and charges at the interfaces will vibrate under the influence of the Coulomb force, producing acoustic waves. Next, the acoustic waves will propagate along the thin axis of the sample and are captured by a piezoelectric sensor (PVDF, PolyVinylidene Difluoride Film) tightly attached to the bottom electrode. The voltage waveform collected by the oscilloscope is the electrical signal converted from the vibration signal of the PVDF sensor. Therefore, a corresponding quantitative relationship between the voltage signal and the distribution of space charges needs to be established. This is the main mission in the calibration stage [3], [4].

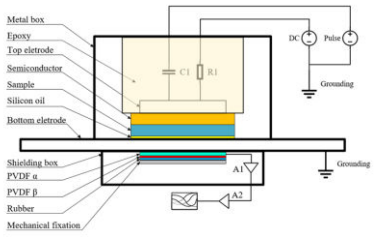

Fig. 1. Schematic of the PEA setup

II. Signal Distortion

In the calibration stage, a low polarization voltage will be applied to a space-charge-free sample. If the flat sample does not contain any space charge inside, the charges accumulated on the contact surface between the sample and the two electrodes, after applying polarization voltage, should be equal but of different polarities according to the laws of charge conservation and Gauss's law (shown in Fig. 2). As the amplitude of the output voltage signal should be proportional to the space charge density, the voltage signal should contain two pulse waves with the same amplitude but opposite polarity. However, as Fig. 2 shows, the measured voltage signal is distorted by overshoot, attenuation, and dispersion [5], [6], [7].

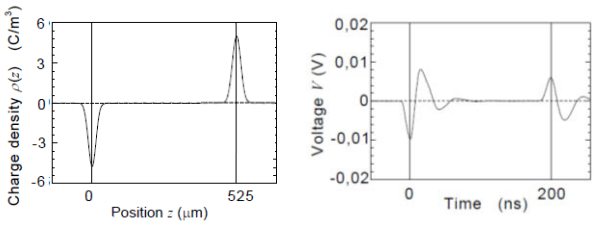

Fig. 2. Comparison between ideal and actual output waveform

A. Overshoot

Fig. 2 shows that each waveform is followed by a distinct oscillation, which is the result of the frequency response of the combination of the PVDF sensor and amplifiers[4]. Fig. 3.a shows the equivalent circuit of the sensor-amplifier combination. Here, C_{sensor} is the capacitance of the PVDF sensor, U_{sensor} is the voltage from the sensor, and $R_{amplifier}$ is the input resistance of the amplifier [3], [8].

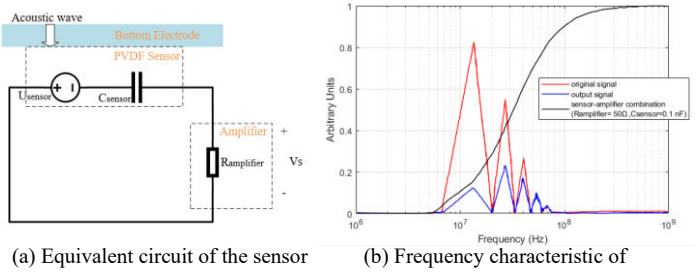

(a) Equivalent circuit of the sensor amplifier combination (b) Frequency characteristic of different systems or signals

Fig. 3. Sensor-amplifier combination and its frequency characteristic

The cutoff frequency of this combination can be expressed by Eq. 1. According to the value of $R_{amplifier}$ and C_{sensor}, the combination of sensor and amplifier can be regarded as a high-pass filter, which allows more high-frequency components of the acoustic signal to be present [8].

$$f_{cutoff} = \frac{1}{2\pi R_{amplifier} C_{sensor}} \quad (1)$$

979-8-3315-8902-8/25/$31.00 ©2025 European Union

Fig. 3.b shows that the filter significantly attenuates the low-frequency components while it allows high-frequency components to pass with virtually no attenuation. This causes the overshoot and undershoot combination issue observed on the captured waveforms.

B. Attenuation and dispersion

Apart from the overshoots, it can be observed that the amplitude of the second pulse is lower than that of the first one in Fig. 2. This attenuation is caused by the attenuation and dispersion effects of the dielectric sample on acoustic waves propagating inside the insulation [5]. Taking a flat sample as an example, when a polarization voltage and excitation voltage are applied, the acoustic waves (*p1* and *p2*) caused by charge vibration will propagate to both sides. In the positive direction of the x-axis, on one side of the PVDF sensor, *p1* will pass through the metal electrode to reach the sensor, while *p2* needs to pass through the flat sample and the metal electrode and bounce back to reach the sensor (shown in Fig. 4). Compared with insulation materials, metals are excellent conductors of acoustic waves due to their high density and an excellent modulus of elasticity, but the loss of acoustic waves in dielectrics is significant due to their absorption and scattering. That is why the second pulse signal magnitude is lower than the first.

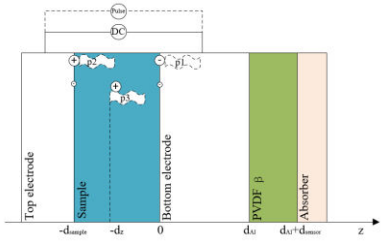

Fig. 4. Propagation of the acoustic wave

III. ADDRESSING OVERSHOOT

The overshoot phenomenon in the signal is often considered a systematic error of the measurement equipment. The commonly used method to eliminate this error is deconvolution [4],[9],[10]. In the PEA system, the output voltage signal $u_s(t)$ can be represented by the convolution of the system's impulse response function $h(t)$ and the space charge density function $\rho(t)$ (shown in Eq. 2).

$$u_s(t) = h(t) * \rho(t) = \int_{-\infty}^{+\infty} h(t-\tau)\rho(\tau)d\tau \quad (2)$$

Complex convolution operations in the time domain can be converted into multiplication and division operations in the frequency domain through FFT (Fast Fourier Transform). The expression of Eq. 2 in the frequency domain is shown in Eq. 3. $H(f)$ is called the system's transfer function.

$$U_s(f) = H(f)R(f) \quad (3)$$

Therefore, $R(f)=U_s(f)/H(f)$. Once $H(f)$ is determined, the space charge distribution can be obtained through a deconvolution operation. In this case, a reference signal $\rho_0(t)$ is introduced. A similar relationship between this reference signal and its output can be expressed by Eq. 4.

$$U_r(f) = H(f)R_0(f) \quad (4)$$

From Eq. 3 and Eq. 4, the expression of $R(f)$ can be obtained:

$$R(f) = \frac{R_0(f)U_s(f)}{U_r(f)} \quad (5)$$

Since $U_s(f)$ is known in Eq. 5, securing a suitable reference signal is key to getting $R(f)$. The signals generated by two typical kinds of charges have been studied and used as reference signals (shown in III.A and III.B).

A. Interface charges between flat sample and bottom electrode

Typically, the induced interfacial charge between the flat sample and the lower electrode is chosen as the reference signal because, theoretically, the thickness of this layer of charge is infinitely thin, so that it can be regarded as an impulse function. The measured voltage signal, which is the first pulse of the output voltage, is the pulse response function of the system [9],[11],[12].

However, when space charge is present inside the sample, the induced charge at the boundary may change. Therefore, when calculating the impulse response function of the test system, the sample should not contain any space charge. Therefore, a lower electric field that does not cause accumulation of space charge is used. When calculating, it should be noted that the induced interface charge density is the surface charge density (C/m^2) (shown in Fig. 5).

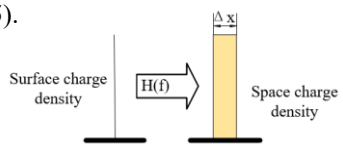

Fig. 5 Interface charge between a flat sample and bottom electrode

Due to the sampling time limitation using a digital oscilloscope for testing, the measured signal is discrete data with a time interval of Δt. Therefore, the induced charge surface density $\sigma(0)$ needs to be discretized and simplified into a distribution with a bulk density of $\rho(0)$, as shown in Eq. 6.

$$\rho(0) = \frac{\sigma(0)}{v_{sa}\Delta t} \quad (6)$$

In Eq. 6, v_{sa} stands for the velocity of the acoustic wave inside the dielectric material.

The advantage of this traditional method is obvious: it is easy to implement. However, considering that most electrodes form an acoustic inhomogeneity, the acoustic wave at the interface can be different from the pulse travelling through the bulk. Moreover, it is assumed that there will be no accumulation of space charges when applying a low polarization voltage, but space charges might already be present inside the sample. This would significantly degrade the accuracy of the measurement.

B. Improved three-layer calibration sample

To improve the traditional reference signal, a new calibration sample with a very narrow bulk charge density was made from an internal gold electrode included in a 2mm layer of PMMA (PolyMethylMethAcrylate) (shown in Fig. 6) [13], [14]. The gold layer is sufficiently thin (much thinner than PMMA) so as not to affect the acoustic properties of the sample. A DC voltage applied on the gold layer generates a charge layer, the density of which can be calculated if the capacitance between the gold layer and the electrodes is known. The gold layer will be connected to the high-voltage electrode, enabling accurate calculation of capacitance.

979-8-3315-8902-8/25/$31.00 ©2025 European Union

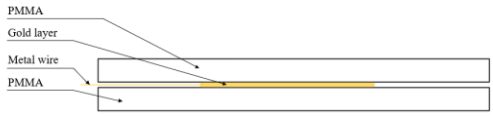

Fig. 6 Flat sample with a thin gold layer

As this structure is a dual-layer dielectric sample, their mutual capacitances must be considered when calculating the charge density on the gold layer. Based on this, an improved calibration procedure was made by building a capacitance matrix to improve the calibration accuracy [15].

The two presented methods introduce the selection of reference signals for flat specimens. By solving for the reference signal, the distribution of the original space charge can be obtained. However, when the sample becomes a full-scaled cable, some changes occur. Firstly, in full-size specimens, multiple reflections produce long and complex signal tails. Truncating these tails with window functions before FFT distorts the spectrum. Secondly, cable samples without space charges are harder to obtain. Solutions to these issues will be discussed in III.C and III.D.

C. Laplace – domain deconvolution method

In the case of film samples, its good impedance matching allows signals to be properly extracted in the region across the thickness of the insulator. Therefore, the signal is appropriate for deconvolution using the FFT because its head and tail converge to zero. By contrast, full - scale cables exhibit long, multi - reflection tails from impedance mismatches in the insulation, so windowing before the Fourier transform truncates critical low - frequency content and produces distorted baselines after deconvolution [7]. The Laplace transform offers a robust alternative for transient - response deconvolution. By multiplying the time domain signal by an exponential $e^{-t/\tau}$, the Laplace transform naturally suppresses long tail components without hard windowing. After dividing in the Laplace domain and then removing the exponential weight, one recovers accurate short - time behaviour governed by the chosen time constant τ, while long - time noise amplification is controlled. As τ increases, the Laplace transform approaches the Fourier transform, so an optimal τ balances tail suppression and spectral fidelity preserving causality and avoiding "division by zero" artifacts that plague FFT deconvolution.

The Laplace transform is represented as:

$$L\{s(t)\} = \int_0^\infty s(t) \exp\left(-\left(\frac{1}{\tau} + j\omega\right) t\right) dt \tag{7}$$

where τ is the time constant, and ω is the angular frequency. It is equivalent to the Fourier transform when τ is very large. Fig. 7 shows the processing difference between Fourier and Laplace deconvolution.

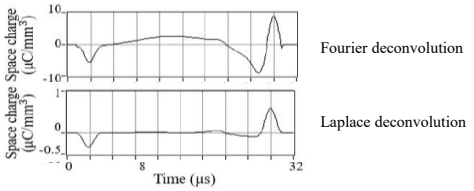

Fig.7. Comparison of the results by Fourier and Laplace deconvolutions

D. Correction of reference signals with a full-scale cable sample containing space charges

Similar to traditional planar samples, the reference signal for measuring the space charge of full-scale cables also uses the interface charge between the cable sample and the bottom electrode. However, preparing space-charge-free cable samples is much more expensive and complex. Furthermore, in measurement of extra-high voltage cables and other real-scale insulation systems, there are many cases when space charge was already produced through charging and thermal operation history; thus, reference signals must be acquired in a full-scale cable sample containing space charges.

The existence of space charges inside the insulation layer brings back an old problem: the presence of space charges can affect the amplitude of the interface charges, leading to inaccurate reference signals. To solve this problem, a method that extracts reference signals by capturing differential acoustic waveforms resulting from two distinct polarization voltages was proposed [16],[17]. When bias voltage u_b and pulsed voltage u_p are applied between the electrodes, there is no space charge, the electric field is as shown in Eq. 8.

$$\frac{\varepsilon}{2}E^2(t) = \frac{\varepsilon}{2d}\left[u_b + u_p(t)\right]^2$$
$$\frac{\varepsilon}{2}E^2(t) = \frac{\varepsilon}{d}\left[\frac{1}{2}{u_b}^2 + u_b u_p(t) + \frac{1}{2}{u_p}^2(t)\right] \tag{8}$$

In Eq. 8, d is the thickness of the insulation layer. The first term on the right-hand side is a constant that does not cause any charge vibration. The third term is too small compared to the second term and can be ignored, so the second term is the only one that truly affects the acoustic wave output.

If space charge exists, it is difficult to separate a signal generated by the space charge from the reference signal used for calibration; however, when the difference between two different bias voltages, u_{b0} and u_{b1}, is taken, Eq. 9 is obtained because the signal component due to space charge does not depend on the bias voltage.

$$\Delta f = \frac{\varepsilon}{d}[u_{b0} - u_{b1}]u_p(t) \tag{9}$$

This signal is proportional to the pulsed voltage. Here, the differential waveform in response to the bias voltages u_{b0} and u_{b1} is multiplied by $u_{b0}/(u_{b0} - u_{b1})$ to determine reference signal $S_{ref}(t)$ under reference voltage u_{b0}, which is expressed in Eq. 10.

$$S_{ref}(t) = u_{b0}u_p(t) * h(t) \tag{10}$$

IV. Addressing Attenuation and Dispersion

After deconvolution processing, the overshoots are removed from the distribution signal. The waveform should be as shown in Fig 8. However, as mentioned in Section II.B, the amplitude and width of the second pulse have changed compared to the first due to the attenuation and dispersion of the acoustic signal in the dielectric. The purpose of calibration is to restore the waveform to its undistorted state.

In the time domain, the expression for waves passing through a medium can be expressed as [5]

$$p(t,z) = p_0 e^{-\alpha z} \cdot e^{-j(wt-\beta z)} \tag{11}$$

where p_0 stands for the original waveform, $p(t,z)$ stands for the waveform at the specific time and location, α is the attenuation

979-8-3315-8902-8/25/$31.00 ©2025 European Union

coefficient, and β is the dispersion coefficient. From Eq.8, it can be seen that α and β modify the amplitude and phase of the original waveform.

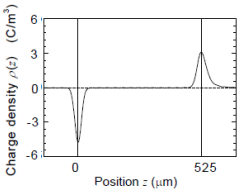

Fig. 8. Space charge distribution after deconvolution

In the frequency domain, a similar equation can be obtained:

$$p(f,z) = p(f,0)e^{-\alpha(f)z} \cdot e^{-j\beta(f)z} \quad (12)$$

From Eqs. 11 and 12, as long as the attenuation coefficient α and dispersion coefficient β are obtained, the waveform before attenuation can be smoothly restored. According to the related definition, the transfer function of the dielectric system can be obtained using Eq. 12:

$$g(f,z) = \frac{p(f,z)}{p(f,0)} = e^{-\alpha(f)z}e^{-j\beta(f)z} \quad (13)$$

For ease of calculation, Gaussian functions can be used to fit the two waveforms obtained in Fig. 9. In this case,

$$\alpha(f) = \frac{-1}{d} ln\left[\frac{|P(f,d)|}{|P(f,0)|}\right] \quad (14)$$

$$\beta(f) = \frac{1}{d} ln[\Phi(f,d) - \Phi(f,0)] \quad (15)$$

By substituting Eqs. 14 and 15 into Eq.13 and performing an inverse FFT, the time-domain transfer function of the dielectric system at each position can be obtained.

$$G(t,z) = [g(t,z_1), g(t,z_2), \dots, g(t,z_{n-1}), g(t,z_n)] \quad (16)$$

Where n stands for the n sampling points. The quantitative relationship between the output voltage and the actual space charge can be easily obtained from the above derivation:

$$\begin{bmatrix} p(1) \\ p(2) \\ . \\ . \\ . \\ p(n) \end{bmatrix} = \begin{bmatrix} g(1,1)\ g(1,2) \cdots g(1,n) \\ g(2,1)\ g(2,2) \cdots g(2,n) \\ . \\ . \\ . \\ g(n,1)\ g(n,2) \cdots g(n,n) \end{bmatrix} \begin{bmatrix} \rho(1) \\ \rho(2) \\ . \\ . \\ . \\ \rho(n) \end{bmatrix}$$

However, matrix calculations may have varying degrees of error due to ill-conditioned problems, which needs to be eliminated further.

V. Conclusions

The current calibration method can obtain measurement data before distortion and find the quantitative relationship between the output voltage and the actual distribution of space charges. However, due to the use of different reference signals, there are differences in the accuracy of removing overshoots. At the same time, when eliminating the impact of attenuation, matrix calculations may have varying degrees of error due to ill-conditioned problems, which need to be further eliminated.

The next challenges to further improve this work are:

1) improve calibration samples

The double-layer sample structure mentioned in section III.B can provide a stable reference signal, but it is difficult to control the casting thickness when preparing the samples. Therefore, an inexpensive and easily manufactured calibration sample should be realized.

2) develop a versatile signal-processing platform

Signal processing is inherently complex and labor‐intensive. To address this, a comprehensive, commercially viable software panel that streamlines the workflow should be developed. The platform should be capable of processing measurement data for various geometries (flat plate, full-scale cable) while providing adjustable parameters to accommodate varying experimental conditions. A flexible, unified interface reduces the time and effort required for data analysis and ensures reliable, reproducible, and representative results across different specimen types and test conditions.

Acknowledgments

This work was supported by the China Scholarship Council under Grant 202209110018.

References

[1] G. Ala *et al.*, "Review of acoustic methods for space charge measurement," in *2015 AEIT International Annual Conference (AEIT)*, Oct. 2015, pp. 1–6.
[2] *A. Ghassemi, "PEA Method Space Charge Measurement, modeling & measurement of applied pulsed-voltage in different setups for MV mini-cable," 2020,* Accessed: May 19, 2023.
[3] M. J. P. Jeroense, "Charges and Discharges in HVDC Cables - in particular in mass-impregnated HVDC cables," 1997, Accessed: Apr. 03, 2023.
[4] "NEN Connect - IEC/TS 62758:2012 en." Accessed: Apr. 24, 2023.
[5] Y. Tanaka, K. Hanawa, K. Suzuki, and T. Takada, "Attenuation recovery technique for acoustic wave propagation in PEA method," in *Proceedings of 2001 International Symposium on Electrical Insulating Materials (ISEIM 2001). 2001 Asian Conference on Electrical Insulating Diagnosis (ACEID 2001). 33rd Symposium on Electrical and Ele*, Nov. 2001, pp. 407–410.
[6] X. Li, T. Kawashima, Y. Murakami, and N. Hozumi, "Acquisition of calibration signal in space charge measurement by pulsed electrostatic method," in *2022 IEEE International Conference on High Voltage Engineering and Applications (ICHVE)*, Sep. 2022, pp. 1–4.
[7] A. Yeongguk, X. Li, T. Kawashima, Y. Murakami, and N. Hozumi, "Signal Processing for Space Charge Measurement Using Laplace Deconvolution," in *2022 9th International Conference on Condition Monitoring and Diagnosis (CMD)*, Nov. 2022, pp. 811–814.
[8] P. Morshuis and M. Jeroense, "Space charge measurements on impregnated paper: a review of the PEA method and a discussion of results," *IEEE Electrical Insulation Magazine*, vol. 13, no. 3, pp. 26–35, May 1997.
[9] K. Hencken and A. Abbasi, "Analysis of the deconvolution and reconstruction of PEA signals for HV insulation materials," in *2016 IEEE International Conference on Dielectrics (ICD)*, Jul. 2016, pp. 926–929.
[10] H. Hussaini, A. A. Adam, and A. A. Susan, "Review of Space-charge Measurement using Pulsed Electro- Acoustic Method: Advantages and Limitations," vol. 5, no. 4, 2015.
[11] R. Bodega, "Space charge accumulation in polymeric high voltage DC cable systems," 2006, Accessed: Nov. 13, 2023.
[12] R. Bodega, P. H. F. Morshuis, and J. J. Smit, "Space charge measurements on multi-dielectrics by means of the pulsed electroacoustic method," *IEEE Transactions on Dielectrics and Electrical Insulation*, vol. 13, no. 2, pp. 272–281, Apr. 2006.
[13] J. T. Holboll, M. Henriksen, and J. Hjerrild, "Dielectric sample with narrow bulk charge distribution," in *ICSD'01. Proceedings of the 20001 IEEE 7th International Conference on Solid Dielectrics (Cat. No.01CH37117)*, Jun. 2001, pp. 493–496.
[14] J. T. Holboll, M. Henriksen, and C. Rasmussen, "Dielectric sample with two-layer charge distribution for space charge calibration purposes," in *Annual Report Conference on Electrical Insulation and Dielectric Phenomena*, Oct. 2002, pp. 648–651
[15] H. Ren, Q. Li, and Z. Wang, "An Improved Calibration Method for the Measurement of Space Charge Inside Insulating Materials," *IEEE Transactions on Instrumentation and Measurement*, vol. 69, no. 4, pp. 1652–1663, Apr. 2020.
[16] X. Li, T. Kawashima, Y. Murakami, and N. Hozumi, "Basic study on calibration using waveform variation in space charge measurement by pulsed electroacoustic method," *Electrical Engineering in Japan*, vol. 216, no. 2, p. e23436, 2023.
[17] X. Li, T. Kawashima, Y. Murakami, N. Hozumi, and P. Morshuis, "Calibration for Pulsed Electroacoustic Space Charge Measurement Using Frequency-Resolved Analysis," *IEEE Transactions on Dielectrics and Electrical Insulation*, vol. 32, no. 2, pp. 797–804, Apr. 2025.

979-8-3315-8902-8/25/$31.00 ©2025 European Union